ASSESSING THE POTENTIAL OF *Caesalpinia Bonducella* LEAF *Ethanol* EXTRACT IN 1M H_2SO_4 SOLUTION FOR CORROSION INHIBITION AND ADSORPTION

[2]Akinjokun, A. I, [1]Oyewumi M. S., [1]Oladele E. P., [1]Esho, J. I., [3]Adeniyi B. O., [1]Olasehinde E. F.

[1]Department of Chemistry, The Federal University of Technology, Akure, Nigeria

[2]Department of Chemical Sciences, Joseph Ayo Babalola University, Ikeji Arakeji , Nigeria

[3]Department of Chemical Science and Technology, Federal Polytechnic Ede, Nigeria

Correspondence
epoladele@futa.edu.ng,
peaceademme@live.com

ABSTRACT

The corrosion inhibition and adsorption properties of Caesalpinia bonducella leaf ethanol (CBLE) extract, a low-cost and sustainable corrosion inhibitor on low-carbon steel coupon in 1M H_2SO_4 solution were studied using weight loss and potentiodynamic polarization measurements. The surface morphology and the organic functional moieties of the extract were obtained from Scanning Electron Microscopy (SEM) and Fourier Transform Infrared spectroscopy (FTIR) data, respectively. The highest Inhibition efficiencies of 73.34% and 82.35% were obtained at 303K and 343K, respectively and at 0.8 g/L extract concentration. Corrosion inhibition occurred by the formation of CBLE extract adsorption films onto the coupon's surface. The adsorption process can be best described by the Langmuir isotherm and chemisorption mechanism. Thermodynamic studies further showed that corrosion inhibition of the steel coupons in an acidic solution mediated by CBLE extract is endothermic and spontaneous. Electrochemical studies showed that the extract is adaptable in that it acts as a mixed-mode inhibitor with a prevalence of cathodic effectiveness

Keywords: *Caesalpinia bonducella, Corrosion, Mild Steel, Electrochemical, Gravimetric, Inhibition.*

History
Received: 31/12/2024
Accepted: 26/03/2025
Published: 30/05/2025

1 | Introduction

In many industrial chemical processes, particularly those associated with the use of acidic electrolytes/solutions, corrosion of metallic components has been identified as a major cause for concern due to its associated negative economic and environmental impacts (Buchweishaija, 2009). These concerns are related to the cost of replacement or repairs of corroded components and the release of potentially toxic metal ions into the environment. To prevent these problems, a diminutive amount (Singh *et al.*, 2011) of a certain class of chemicals called "corrosion inhibitors" is added to the metal's surfaces (Cao *et al.*, 2022; Loto *et al.*, 2021). Corrosion inhibitors are organic compounds containing abundant pie bond systems and heteroatoms which allow them to bind to the metal surface through the formation of a thin film adsorption layer (Pandey *et al.*, 2018; Hijazi *et*

https://www.futa.edu.ng

JOSTIR
JOURNAL OF SCIENCE, TECHNOLOGY AND INNOVATION RESEARCH
https://www.jostir.futa.ng

https://doi.org/10.51459/jostir.2025.1.1.04

al., 2015). Although chemical inhibitor formulations with high inhibition efficiencies are commercially available, their use is limited by high cost and toxicity (Ng *et al.*, 2022; Verma *et al.*, 2018). As a result, many research efforts are currently centered on finding affordable inhibitors made from sustainable feedstock. Several studies have reported that plant extracts with chemical functionalities similar to those found in conventional chemical inhibitors can function as low-cost, eco-friendly and sustainable corrosion inhibitors –(Arockia *et al.*, 2020; Helen *et al.*, 2014; Miralrio and Espinoza Vázquez, 2020; Olasehinde *et al.*, 2022). Extracts from several plants such as *Datura mete* seed (Sathiya *et al.*, 2014; Singh et al., 2016), *aloe vera* (Singh *et al.*, 2016), *alchornea laxiflora* (Oluwafemi *et al.*, 2019; Olasehinde *et al.*, 2015), *Garcinia kola* (Ikeuba *et al.*, 2013) among others have been studied and found to have great potentials as green and low-cost inhibitors.

Caesalpinia bonducella is a shrub (Nallagouni *et al.*, 2021) commonly found growing on its own in the tropics. Its use as an important component of herbal concoctions has been widely documented in the treatment of bacterial and fungal infections; as an anti-diabetic, analgesic, and anti-tumor agent (Billah *et al.*, 2013; Chakrabarti *et al.*, 2005; Pandey *et al.*, 2018; Devi *et al.*, 2008; Kumar *et al.*, 2019; Nazeerullah *et al.*, 2012; Shukla *et al.*, 2009, 2010). The efficacy of plant extract in corrosion inhibition has been reported to be dependent on many variables including the type of corrosion medium, nature of corrosion inhibitors and extracting solvent (Salleh *et al.*, 2021; Hijazi *et al.* (2015). Meanwhile, preliminary investigation showed that *Caesalpinia bonducella* leaf contains some phytochemicals which could make it function as a good corrosion inhibitor. However, literature search reveals that no study has been done on the inhibitive effects of *Caesalpinia bonducella* leaves ethanol extract on acid corrosion of mild steel. Therefore, this study attempts to investigate the inhibitive effects of CBLE on mild steel corrosion in 1M H_2SO_4 solution. It should be noted that despite the effectiveness and relatively low toxicity of ethanol as extractant, care must be taken during the extraction due to its flammability which can pose a fire risk during extraction.

2. | Materials and methods

2.1 | Materials Preparation

Mild steel was obtained from School of Engineering workshop, Oba-kekere, FUTA and the chemical composition was determined at universal steel, Ogba, Lagos State. The mild steel specimen had the following elemental composition of C: 0.215%, Si: 0.258%, Mn: 0.467%, S: 0.009%, Cr: 0.007%, Ni: 0.001%, Cu: 0.017%, Ti: 0.019% and others being Fe: 98.98%. The steel was cut into coupons of dimension ranging from 8 mm to 9 mm in height and 8 mm in diameter. Each coupon was polished mechanically using emery papers, washed thoroughly with distilled water, degreased with ethanol and finally dried at room temperature prior to the corrosion test. The leaves of *Caesalpinia bonduc* were obtained from Aramoko-Ekiti in Ekiti State and authenticated at Crop, Soil and Pest Department, Federal University of Technology, Akure.

2.2 | Preparation of Plant Extract

The leaves of *Caesalpinia bonducella* (LCB) were cut into pieces and washed with distilled water, air-dried, and pulverized into powder using a laboratory blender. The LCB powder was thereafter extracted with ethanol (98% w/v) (1g: 5 mL) for 96 h. The extract was concentrated by evaporating the solvent to dryness on a thermostated water bath at 78 ^{o}C to obtain the *Caesalpinia bonducella* leaf ethanolic (CBLE) extract. Extract with masses ranging from 0.2 – 0.8

https://doi.org/10.51459/jostir.2025.1.1.04

g were weighed and then dissolved separately in 1000 mL 1M H_2SO_4 solution for use as the media for the corrosion study.

2.3 | Characterization

The IR spectrum of the CBLE extract was recorded using a PerkinElmer 1600 FTIR spectrometer (Sehmi et al., 2020). A dried sample (0.5g) of the CBLE extract was powdered with KBr to form IR transparent pellets and used in spectrum collection. The surface morphology of the steel coupon before and after immersion for 4 h at room temperature in the corrosive test media containing 0 % w/v and 0.8 % w/v CBLE extract in 1M H_2SO_4 solution surface was viewed using a Scanning Electron Microscope.

2.4 | Caesalpinia bonducella ethanolic extract corrosion inhibition estimation

2.4.1 | Weight loss measurements

The difference in weights of the steel coupons before and after immersion in corrosion media expressed as weight-loss was utilized in determining the extent of corrosion inhibition – (Cao *et al.*, 2022; Ikeuba *et al.*, 2022; Loto *et al.*, 2021; Sehmi *et al.*, 2020; Wang *et al.*, 2020). Effects of parameters such as CBLE extract concentration (in gL^{-1}) and solution temperature (in Kelvin) on corrosion inhibition were investigated to obtain information on the effectiveness of CBLE extract as a viable inhibitor of corrosion.

The effect of extract concentration was investigated by dipping pre-weighed steel coupon into each of five 250 mL beakers containing 100 mL of 1M H_2SO_4 at 298K for 4 h in addition to 0 % (w/v), 0.2% (w/v), 0.4% (w/v), 0.6% (w/v) and 0.8% (w/v) CBLE extract. The effect of temperature was studied by immersing pre-weighed coupons in 100 mL corrosion media containing 0 % (w/v), 0.2% (w/v), 0.4% (w/v), 0.6% (w/v) and 0.8% (w/v) CBLE extract in 1M H_2SO_4 contained in 250 mL beakers in a thermostated water bath maintained at 303 – 343 K for 4 h. The corrosive test media with 0 %(w/v), and 0.2 – 0.8 % (w/v) CBLE extract is designated as the blank and inhibited solution respectively.

At the end of each experimental run, the steel coupons were retrieved from the acidic media and re-weighed after thorough washing with distilled water and acetone – ' (Umoren *et al.*, 2016). The coupons weight loss data were used to compute corrosion rate, C_R ($mgcm^{-2}.h^{-1}$), inhibition efficiency, η (%), and surface coverage, θ using Eqs. 1-3 (Olasehinde *et al.*, 2022; Sehmi *et al.*, 2020; Verma *et al.*, 2016).

$$C_R = \frac{\Delta w}{At} \qquad (1)$$

where $\Delta w = w_0 - w_1$

$$\eta\ (\%) = \left(1 - \frac{C_{R(inh)}}{C_{R(blank)}}\right) \times 100 \qquad (2)$$

$$\theta = \frac{\eta}{100} \qquad (3)$$

Where A = surface area of the steel coupon (in cm^2*), t = time of steel coupon's immersion in the corrosive media (in sec.), Δw = difference in steel coupon's weight (in g),* w_o*= initial weight of the steel coupon and,* w_1*= weight of steel coupon after immersion in the corrosive media for the stipulated time.*

2.4.2 | Potentiodynamic Polarization (PPP) Curves measurement

Tafel or PPP curves were measured in the blank and solutions containing the extract and recorded at 298 K on a 3 electrodes AUTOLAB PGSTAT 204N system consisting of platinum foil, standard silver/silver chloride electrode and the steel

https://doi.org/10.51459/jostir.2025.1.1.04

coupon (circular with surface area = 1 cm^2) designated as the counter/auxiliary, reference and working electrodes respectively. The curves were recorded between -250 mV and +250 mV (vs, OCP) at a scan rate of 1.0 mV. s^{-1} after the coupon's initial immersion in the acidic media for about 30 minutes. Linear segments of the anodic and cathodic Taffel curves were extrapolated from the corrosion potential (E_{corr}) to obtain the current density (i_{corr}) from which inhibition efficiency (η %) was calculated using Eq.4 (Olasehinde, Agbaffa, Adebayo, & Enis, 2022; Verma *et al.*, 2016)

$$\eta(\%) = \frac{\left(i_{corr_{(blank)}} - i_{corr_{(inh)}}\right)}{\left(i_{corr_{(blank)}}\right)} \times 100\ \% \qquad (4)$$

Where ($i$corr $_{(blank)}$ – $i$corr $_{(inh)}$) is the corrosion current density (in μAcm^{-2}) in the blank and inhibited solution respectively.

3.0 | Results and Discussion

3.1 | Characterization

The FTIR spectrum of CBLE extract is presented in Figure 1a and showed a sharp peak at 3396 cm^{-1} which could be due to O-H or N-H bond stretching vibration. The peaks at 1646 cm^{-1}, 1531 cm^{-1} and 2356 cm^{-1} could be due to C=O, C=C, and C-H bonds stretching vibration in aromatic ring. Furthermore, the peaks at 1117 cm^{-1} could be due to C-O bond stretching vibration of aromatic ether while =C-H and C-H bonds bending vibration could be responsible for peaks < 1000 cm^{-1}. These results indicate that CBLE contains O and N atoms in functional groups (O-H, N-H, C=C, C=N, C=O, C-O) and aromatic ring. These peaks are consistent with those reported for bonducellin (Figure 1b), a major compound isolated from CBLE (Hijazi *et al.*, 2015).

3.2 | Assessment of Weight Loss

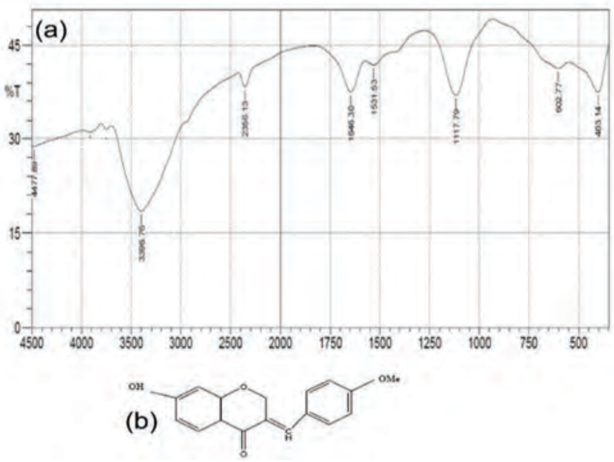

Figure 1 | (a) FTIR spectrum of ethanolic extract of *Caesalpinia bonducella* leaf, and (b) structure of bonducellin, an important compound in CBLE extract

Figures 2a-e show that corrosion rate (C_R) and corrosion inhibition (IE%) vary with CBLE extract concentration and temperature. A significant decrease and increase respectively in the rate of corrosion (C_R) and inhibition efficiency (IE%) is seen with increasing concentrations of CBLE extract (Figures 2a-e). Similar trends have been reported by previous studies (Adebayo *et al.*, 2019a; Olasehinde *et al.*, 2015; Olasehinde *et al.*, 2022; Olasehinde *et al.*, 2022; Singh *et al.*, 2016; Verma *et al.*, 2018). These studies suggest that the observed variation in C_R and IE (%) with increasing concentration of the CBLE extract could be connected to the enhanced adsorption and coverage of the steel coupon's surface with adsorbed films of corrosion-inhibiting natural molecules found in the extract (Salleh *et al.*, 2021).

Though the corrosion rate increased with increasing solution temperature, the rate is nonetheless reduced by the extract (Figure 2). Furthermore, inhibition efficiency (%) increased with increasing solution temperature indicating the propensity of the CBLE extract to inhibit corrosion (Figure 2). Inhibition efficiency increased from 59.41 % at 303 K to 78.72% at 343 K in 0.2 % (w/v), from 63.74 % at 303 K to 80.02% at 343 K in 0.4 % (w/v), from 71.61 % at 303 K to 80.82 at 343

https://doi.org/10.51459/jostir.2025.1.1.04

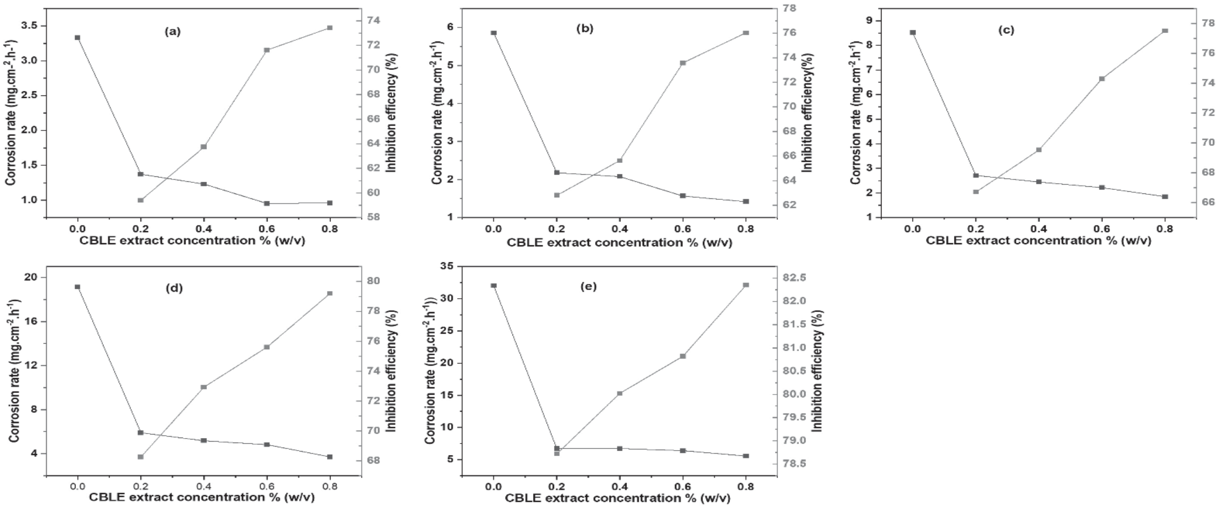

Figure 2 | Variation in corrosion rate and inhibition efficiency with CBLE extract concentration in 1M H_2SO_4 at (a) 303 K, (b) 313 K, (c) 323 K, (d) 333 K, and (d) 343 K

K in 0.6 % (w/v), from 73.43 % at 303 K to 82.35 % at 343 K in 0.8 % (w/v) (Figure 2). This trend may be as a result of increased stability of the adsorbed thin film CBLE extract molecules on the metal surface or association between the metal surface and the adsorbed extract thin film with increasing solution temperature (Sehmi *et al.*, 2020); this trend has been ascribed to chemisorption (– Devi *et al.*, 2020; Sehmi *et al.*, 2020; Umoren *et al.*, 2018; and Verma *et al*, (2016).

Figures 3 (a) – (c) shows the SEM images of the steel coupon surface before and after immersion in the corrosion media. The unevenness of the steel coupon surface morphology (Figure 3(b)) attests to the aggressive attack by the blank acidic solution. In contrast, the surface morphology of steel coupon immersed in the inhibited corrosion medium (Figure 3c) is noticeably preserved thus implying that CBLE extract significantly reduces

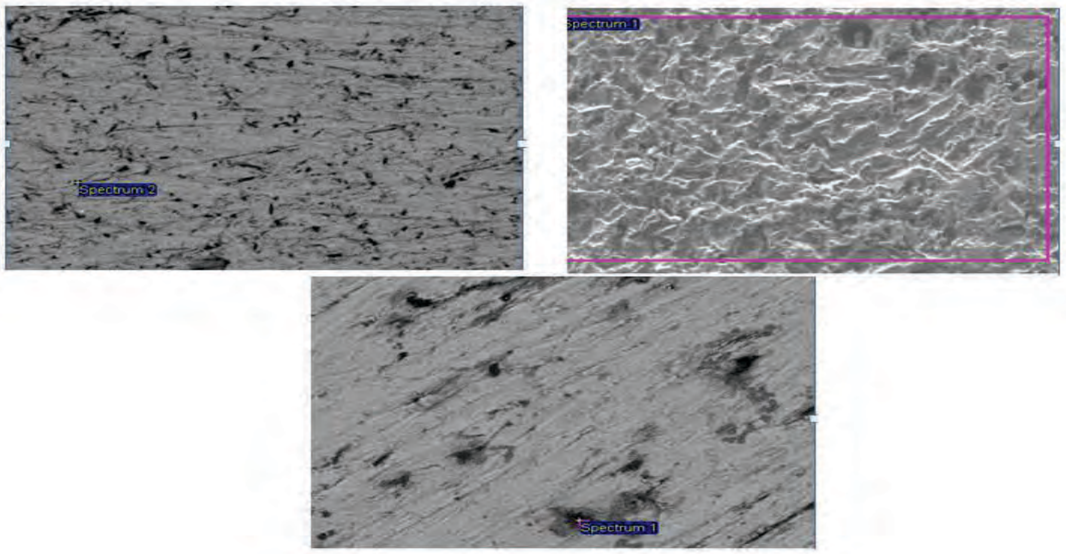

Figure 3 | SEM Images of steel coupon (a) before immersion in blank and inhibited, (b) after immersion in blank, and (c) after immersion in inhibited solutions

https://doi.org/10.51459/jostir.2025.1.1.04

or inhibits corrosion.

3.3 | Adsorption isotherm and thermodynamic

3.3.1 | Adsorption isotherms

Surface coverage data obtained from the weight-loss experiments were fitted to Freundlich, Langmuir, and Temkin isotherm models. According to Langmuir isotherm model, the adsorption of inhibitor molecules is by monolayer adsorption onto uniform sites of the steel coupons surface. The adsorbed inhibitor molecules do not interact with one another (Akinjokun *et al.*, 2023; Oladipo *et al.*, 2021). The linear version of the Langmuir isotherm equation is depicted in Eq.5 (Akinjokun *et al.*, 2023; Oladipo *et al.*, 2021) :

$$\frac{C_{inh.}}{\theta} = \frac{1}{K_{ads}} + C_{inh.} \qquad (5)$$

where C_{inh} is the concentration of CBLE extract; K_{ads} represents the equilibrium adsorption constant while θ is the surface coverage of steel coupon with the CBLE extract (inhibitor). Estimation of K_{ads} at different inhibitor concentrations was determined from the intercepts $\left(\frac{1}{K_{ads}}\right)$ of $\frac{C_{inh.}}{\theta}$ versus C_{inh} (Figure 4a).

Freundlich isotherm model, an empirical model for systems with heterogenous surfaces presupposes that the inhibitor (CBLE extract) adsorbs to various sites with different affinities (Akinjokun *et al.*, 2023). The Freundlich isotherm linear expression is as shown in Eq. 6:

$$log\ \theta = logK_f + \frac{1}{n}\log C_{inh} \qquad (6)$$

where θ = surface coverage, C_{inh} = concentration of inhibitor, K_{ads} and n (dimensionless) are characteristic Freundlich's isotherm constants related to the intensity and capacity of adsorption. The values of n and K_f was calculated from the slope, and intercept of *log* θ versus *log* C_{inh} plots (Figure 4b).

According to Temkin's isotherm, adsorbent and adsorbate interactions cause the heat of adsorption to drop linearly with adsorbent surface coverage (Musah *et al.*, 2022). The Temkin isotherm linearized equation is depicted by Eq. 7:

$$\theta = BlnA_T + BlnC_{inh} \qquad (7)$$

where $B = \frac{RT}{b_T}$; C_{inh} = concentration of the inhibitor (CBLE); θ = surface coverage; b_T and A_T are respectively Temkin's heat constant of adsorption ($J.mol^{-1}$) and isotherm ($L^{-1}.\ g$) while R and T = gas constant (8.314 $J.mol^{-1}.\ K^{-1}$) and absolute temperature (in K) respectively. Temkin's constants, b_T and A_T were estimated from the slope and intercept of θ versus ln C_{inh} plots (Fig. 4c).

The goodness of fit of experimental data to the applied models was confirmed using the coefficients coefficient (R^2) proximity to unity (Oladipo *et al.*, 2021). Examination of the estimated values of the coefficients coefficient (R^2) obtained from Fig. 4 as shown in Table 1 revealed that Langmuir's isotherm with the highest R^2 values ranging from 0.9951 to 0.9976 (Table 1) provides the best fit for the data. It could also be observed from the Table that the values of Kads increase with increasing temperature which suggest a strong adsorption interaction between the extracts and the mild steel surface in 1M H_2SO_4 solution. Further, an increase in k_f and b with increasing temperature suggest an endothermic adsorption process, where heat is absorbed during adsorption. (Salleh *et al.*, 2021; Verma *et al.*, 2016; Wang *et al.*, 2020; Sehmi *et al.*, 2020; Umoren *et al.*, 2018).

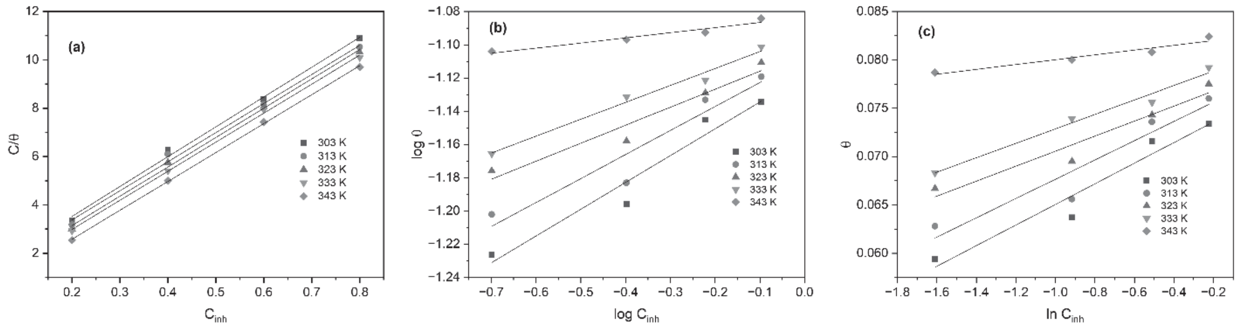

Figure 4 | (a) Langmuir, (b) Freundlich and, (c) Temkin adsorption plots

Table 1 | Estimated values of coefficient coefficient (R^2) and calculated parameters for Langmuir, Freundlich and Temkin adsorption plots

	Langmuir isotherm		Freundlich isotherm		Temkin isotherm		
Temp.(K)	Kads	R^2	b (kJ/mol)	R^2	k_f	1/n	Intercept
303	9.46	0.9963	17.15	0.9495	0.083	0.161	0.9424
313	10.30	0.9951	19.62	0.9117	0.094	0.144	0.9048
323	14.08	0.9976	26.34	0.9432	0.105	0.108	0.9354
333	16.12	0.9988	28.35	0.9812	0. 108	0.103	0.9791
343	54.73	0.9997	77.68	0.9366	0. 118	0.030	0.9330

3.3.2 | Thermodynamic parameters

Furthermore, the thermodynamic parameter, ΔG^o_{ads} for the adsorption of CBLE extract was determined at the studied temperatures from Eq.8 (Adebayo *et al.*, 2019b):

$$\Delta G^o_{ads} = -RT ln(55.5 * K_{ads}) \tag{8}$$

The estimated values of ΔG^o_{ads} at the studied temperatures are all negative and varied from -22.74 kJ.mol^{-1} to -45.58 kJ.mol^{-1} (Table 2) and confirms that CBLE extract corrosion inhibition occur spontaneously (Olasehinde *et al.*, 2022; Kumar & Mohana, 2014). Adsorption processes are frequently classified as physisorption or chemisorption based on the values of ΔG^o_{ads} process with ΔG^o_{ads} values ≤ 20 kJ.mol^{-1} and between -20 kJ.mol^{-1} and -40 kJ.mol^{-1} are classified respectively as physisorption and chemisorption – (Olasehinde *et al.*, 2022; Umoren *et al.*, 2018; Verma *et al.*, 2016). Therefore, the adsorption of CBLE extract to the metal surface (Table 2) can be said to occur through a chemisorption process which involves the formation of chemical bonds

Table 2 | Calculated CBLE extract adsorption parameters

Temperature (K)	K_{ads} (mol. L^{-1})	ΔG^o_{ads} (kJ.mol^{-1})	ΔH^o_{ads} (kJ.mol^{-1})	ΔS^o_{ads} (J.mol^{-1}. K^{-1})
303	9.46	-22.74	+33.76	-164.70
313	10.30	-24.38		
323	14.08	-28.45		
333	16.12	-31.58		
343	54.73	-45.58		

between the extract and the metal surface via charge transfer (Sehmi *et al.*, 2020; Verma *et al.*, 2018).

Adsorption enthalpy, ΔH^o_{ads} was computed from Van't Hoff thermodynamic model (Eq. 9) (Umoren et al., 2016):

$$\ln K_{ads} = \frac{-\Delta H^o_{ads}}{RT} + Constant \qquad (9)$$

where K_{ads} = equilibrium adsorption constant (mol. L^{-1}) and ΔH^o_{ads} = enthalpy of adsorption (kJ.mol^{-1}) under the specific conditions highlighted in this study.

An estimated ΔH^o_{ads} value of +33.76 kJ.mol^{-1} was obtained (Table 2) from the slope of ln K_{ads} versus 1/T linear plot (Figure 3a) for CBLE extract adsorption unto the metal surface. According to the literature, processes with ΔH^o_{ads} values > 0 are endothermic and attributable to chemisorption whereas processes with ΔH^o_{ads} < 0 are exothermic and could occur either by physisorption, chemisorption, or a combination of the two processes (Jafari *et al.*, 2013), The endothermic nature of the adsorption of CBLE extract is demonstrated by the positive values of positive ΔH^o_{ads} (Table 2). To further understand the relationship between temperature and CBLE extract corrosion inhibition capacity, estimation of activation energy, E_a is necessary (Ansari & Quraishi, 2018). E_a for the adsorption of CBLE extract in corrosion inhibition was evaluated from Eq. 10 –'(Umoren *et al.*, 2016):

$$\ln C_R = \frac{-E_a}{RT} + \ln A \qquad (10)$$

where A = Arrhenius pre-exponential constant. The linear relationship exhibited in ln C_R versus 1/T plots confirms that a linear relationship exists between corrosion rate and temperature (Fig. 5b). In this study, E_a is lower in the inhibited (with CBLE extract) compared to the blank test media (Table 3).

According to Eddy *et al.* (2009), chemisorption and physisorption are typically credited with the inhibition process in which the activation energy values in inhibited solutions are respectively lower than, and higher than in the blank test media. Therefore, CBLE extract-mediated corrosion inhibition investigated in this study could be

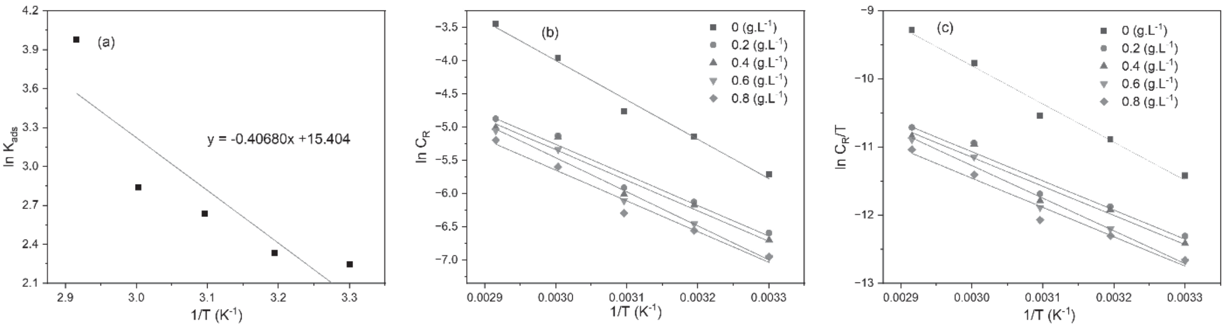

Figure 5 | Plot of (a) $lnK_{ads}\ versus\ \frac{1}{T}$; $(b)\ \ln C_R\ versus\ \frac{1}{T}$, $and\ ln\left(\frac{C_R}{T}\right)\ versus\ \frac{1}{T}$ **for the corrosion inhibition CBLE extract in 1M H_2SO_4 solution.**

Table 3 | Thermodynamic CBLE extract adsorption activation parameters

$C_{inh}(g.L^{-1})$	$E_a(kJ.mol^{-1}K^{-1})$	$\Delta H^*(kJ.mol^{-1})$	$\Delta S^*(J.mol^{-1}K^{-1})$	$E_a - \Delta H\ (kJ.mol^{-1})$	$Q_{ads}(kJ.mol^{-1})$
Blank	49. 40	46.74	-81.37	2.66	-
0.2	36.13	33.44	-132.22	2.68	+17.93
0.4	37.16	34.48	-129.65	2.68	+17.49
0.6	42.39	39.72	-114.47	2.68	+9.64
0.8	38.62	35.95	-127.52	2.68	+10.68

attributed to chemisorption as indicated by CBLE concentration-dependent reduction of the estimated E_a values in the inhibited test media (Table 3).

The CBLE extract-mediated corrosion inhibition activation enthalpy and entropy in 1M H_2SO_4 by was also estimated from Eq. 11:

$$\ln\left(\frac{C_R}{T}\right) = \left[ln\left(\frac{R}{hN_A}\right) + \frac{\Delta S^*}{R}\right] - \frac{\Delta H^*}{RT} \qquad (11)$$

where h = Planck's constant, N_A = Avogadro's number while ΔH^* and ΔS^* is the change in activation enthalpy and entropy. The calculated values of ΔH^* and ΔS^* at different CBLE extract concentrations are enumerated in Table 3. Estimated enthalpy of activation values of +33.44, +34.48, +39.72 and +35.94 $kJ.mol^{-1}$ respectively in the acid test media containing 0.2, 0.4, 0.6 and 0.8 % (w/v) are not significantly different from the standard enthalpy of adsorption (ΔH^o_{ads} = 33.76 $kJ.mol^{-1}$) estimated from Van't Hoff model (Table 3). In addition to this, the positive values of ΔH^* again affirm the earlier claims of the endothermic nature of CBLE extract adsorption unto the metal surface via chemical interactions (Goulart *et al.*, 2013). A closer look at the estimated thermodynamic parameters, E_a and ΔH^* shows that E_a values are generally greater than ΔH^*; this trend is synonymous with corrosion processes accompanied by the release of hydrogen gas – ' (Umoren *et al.*, 2016) associated with a decrease in the solution volume. This also agrees with the thermodynamic relationship described by Eq. 12 (ref.) that there is a difference between the estimated values of Ea and ΔH^* (Table 3):

$$E_a - \Delta H^* = R * T \qquad \mathbf{(12)}$$

The mean of the difference (2.67 k.J.mol^{-1}) is similar to the product of the universal gas constant, R (8.314 Jmol^{-1}K^{-1}) and T (298K) (2.48 kJ.mol^{-1}) (Table 4). Furthermore, ΔS^* decreased with increasing concentration of CBLE extract (Table 4). This is indicative of a decrease in disorderliness on metal surfaces in the inhibited solutions (Essien *et al.*, 2018; Thommes et al., 2015).

3.3 | Potentiodynamic Polarization Measurements

Values of characteristic parameters such as i_{corr}, E_{corr}, β_c a and β_a were obtained by extrapolating the linear portions of the polarization curves (Verma *et al.*, 2016) for the CBLE extract-mediated corrosion inhibition in 1M H_2SO_4 at 298 K (Figure 6) and are presented in Table 6. The corrosion inhibition efficiency of CBLE extract was estimated using Eq. 13:

$$\eta(\%) = \frac{i_{corr(blank)} - i_{corr(inh)}}{i_{corr(blank)}} \; x \; 100 \qquad (13)$$

where $i_{corr(blank)}$ and $i_{corr(inh)}$ is the current density in the blank and inhibited solution with 0.8 g. L^{-1} CBLE extract.

From the results, E_{corr}, i_{corr}, and β_a decreased in value with increasing CBLE extract concentration (Table 4). Corrosion current density (i_{corr}) decreased from 1038 μA.cm^{-2} in the blank test media to 168.2 μA.cm^{-2} in the inhibited test media (Table 4) due to an appreciable suppression of (i) corrosion arising from the dissolution of the metal surface and (ii) the evolution of hydrogen gas on the anodic and cathodic reactions (Helen *et al.*, 2014). The decrease in i_{corr} could also be due to the increase in the adsorption of inhibitor molecules on the surface of the MS thereby inhibiting the transfer of charge from the anodic and cathodic reaction (Olivares et al., 2006). Inhibition efficiency increased from 73% to 83.30% with increasing CBLE extract concentration and decreasing current density (Table 4). Although the corrosion potential E_{corr} decreased with CBLE extract concentration, the decrease observed in E_{corr} values in the inhibited and blank solution decides the mode of inhibition. When the magnitude of shift is greater than 85 mV, it is then inhibition mode is either anodic or cathodic. However, when the shift < 85 mV, inhibition mode is mixed-type. In this study, E_{corr} shift was < 85 mV (Table 4) thus implying that CBLE extract inhibits

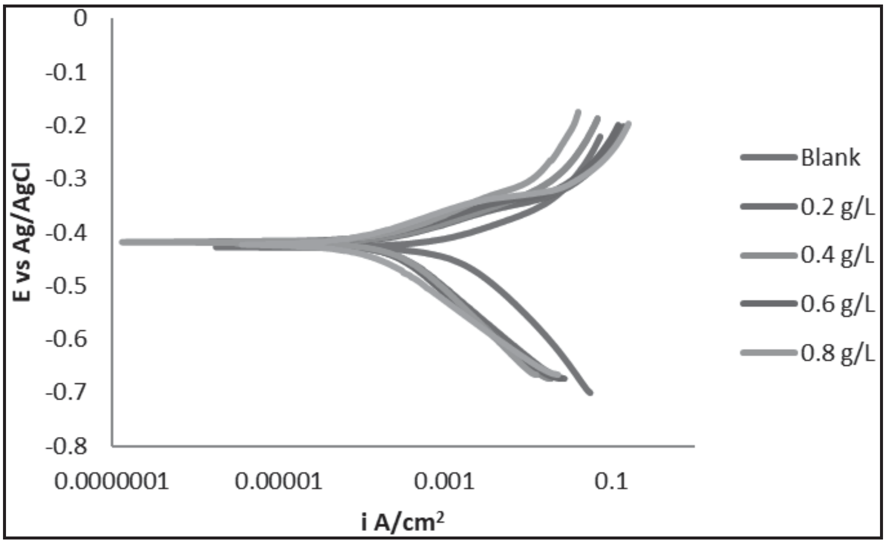

Figure 6 | Potentiodynamic polarization curves for CBLE extract-mediated corrosion inhibition

Table 4 Potentiodynamic polarization parameters for CBLE extract mediated corrosion inhibition in 1M H_2SO_4 solution

C_{inh}(g.L^{-1})	E_{corr} (mV)	i_{corr} (μA.cm^{-2})	β_a (mV.dec^{-1})	β_c (mV.dec^{-1})	C_R (mm.y^{-1})	IE (%)
Blank	-428.7	1038	66.68	120.24	12.06	
0.2	-422.1	273.3	62.43	151.68	3.17	73.00
0.4	-420.5	231.6	55.82	141.18	2.50	77.7
0.6	-471.3	177.5	55.41	123.24	1.91	82.9
0.8	-419.2	168.2	58.28	126.24	2.90	83.8

steel coupon corrosion through deceleration of both cathodic and anodic reactions. However, the higher values of β_c relative to β_a for all extract concentrations (Figure 6) indicates that corrosion inhibition by the extract is predominantly via reduction of cathodic reactions. Thus, CBLE extract can be classified as a dual mode inhibition with mainly cathodic effectiveness (Helen *et al.*, 2014).

4 | Conclusion

This study investigated corrosion inhibition of *Caesalpinia bonducella* leaf ethanolic (CBLE) extract on mild steel coupons in 1M H_2SO_4 using weight loss and potentiodynamic polarization measurements. Corrosion rate decreased with CBLE extract concentration and increased with temperature. The positive values of transition state enthalpy indicate that the corrosion process is endothermic while the negative values of standard entropy are indicative of a decrease in disorderliness at the metal/solution interface. The values of the standard Gibbs free energy, (ΔG^o) ranged from -22.74 kJ.mol^{-1} to -45.58 kJ.mol^{-1}. The mechanism of sorption of CBLE extract to the steel coupon surface is chemisorption. The adsorption of the extract can be described by Langmuir's isotherm while electrochemical measurements showed that CBLE extract has a high cathodic effectiveness.

Acknowledgments

The authors acknowledge the technical assistance provided by the Corrosion Laboratory of the Federal University of Technology, Akure.

Reference

Adebayo, O. L., Olasehinde, E. F., Lajide, L., & Oloruntoba, D. (2019a). *Effect of Drying Method on Phytochemical Compositions and Inhibition Efficiency of Alchornea Laxiflora and Mucuna Flagellepes Leaves Extracts in Corrosion Prevention.*

Adebayo, O. L., Olasehinde, E. F., Lajide, L., &

https://doi.org/10.51459/jostir.2025.1.1.04

Oloruntoba, D. T. (2019b). Comparative analysis of air dried alchornea laxiflora leaves (AALL) extracted with different solvents on corrosion inhibition efficiency of mild steel in acidic media. In *International Journal of Research in Engineering and Innovation* (Vol. 3, Issue 3).

Akinjokun, A. I., Ogunfowokan, A. O., Ajao, J., Petrik, L. F., & Ojumu, T. V. (2023). Template-free conversion of rice husk silica into nano-zeolite X and its application in adsorption of heavy metal ions. *International Journal of Environmental Science and Technology*, 1–12.

Arockia Selvi, J., Arthanareeswari, M., Pushpamalini, T., Rajendran, S., & Vignesh, T. (2020). Effectiveness of vinca rosea leaf extract as corrosion inhibitor for mild steel in 1 N HCl medium investigated by adsorption and electrochemical studies. *International Journal of Corrosion and Scale Inhibition*, *9*(4). https://doi.org/10.17675/2305-6894-2020-9-4-15

Billah, M. M., Islam, R., Khatun, H., Parvin, S., Islam, E., Islam, S. A., & Mia, A. A. (2013). Antibacterial, antidiarrhoeal, and cytotoxic activities of methanol extract and its fractions of Caesalpinia bonducella (L.) Roxb leaves. *BMC Complementary and Alternative Medicine*, *13*. https://doi.org/10.1186/1472-6882-13-101

Buchweishaija, J. (2009). Phytochemicals as green corrosion inhibitors in various corrosive media: a review. *Tanzania Journal of Science*, *35*.

Cao, K., Huang, W., Huang, X., & Pan, J. (2022). Imidazo [1,2-a] Pyrimidine Derivatives as Effective Inhibitor of Mild Steel Corrosion in HCl Solution: Experimental and Theoretical Studies. *Frontiers in Materials*, *9*. https://doi.org/10.3389/fmats.2022.843522

Chakrabarti, S., Biswas, T. K., Seal, T., Rokeya, B., Ali, L., Azad Khan, A. K., Nahar, N., Mosihuzzaman, M., & Mukherjee, B. (2005). Antidiabetic activity of Caesalpinia bonducella F. in chronic type 2 diabetic model in Long-Evans rats and evaluation of insulin secretagogue property of its fractions on isolated islets. *Journal of Ethnopharmacology*, *97*(1). https://doi.org/10.1016/j.jep.2004.10.025

Deepak Pandey, D., Kumar, A., & Pal Jain, A. (2018). Caesalpinia bonducella: A pharmacological important plant. *Pharma Innov. J.*, *7*(12).

Devi, G. N., Unnisa, C. B. N., Roopan, S. M., Hemapriya, V., Chitra, S., Chung, I.-M., Kim, S.-H., & Prabakaran, M. (2020). Floxacins: As mediators in enhancing the corrosion inhibition efficiency of natural polymer dextrin. *Macromolecular Research*, *28*, 558–566.

Devi, R. A., Tandan, S. K., Kumar, D., Dudhgaonkar, S. P., & Lal, J. (2008). Analgesic activity of Caesalpinia bonducella flower extract. *Pharmaceutical Biology*, *46*(10–11). https://doi.org/10.1080/13880200802215776

Eddy, N. O., Odoemelam, S. A., & Odiongenyi, A. O. (2009). Inhibitive, adsorption and synergistic studies on ethanol extract of Gnetum africana as green corrosion inhibitor for mild steel in H2SO4. *Green Chemistry Letters and Reviews*, *2*(2), 111–119.

Essien, E. A., Kavaz, D., Ituen, E. B., & Umoren, S.

https://doi.org/10.51459/jostir.2025.1.1.04

A. (2018). Synthesis, characterization and anticorrosion property of olive leaves extract–titanium nanoparticles composite. *Journal of Adhesion Science and Technology*, *32*(16). https://doi.org/10.1080/01694243.2018.1445800

Goulart, C. M., Esteves-Souza, A., Martinez-Huitle, C. A., Rodrigues, C. J. F., Maciel, M. A. M., & Echevarria, A. (2013). Experimental and theoretical evaluation of semicarbazones and thiosemicarbazones as organic corrosion inhibitors. *Corrosion Science*, *67*. https://doi.org/10.1016/j.corsci.2012.10.029

Helen, L. Y. S., Rahim, A. A., Saad, B., Saleh, M. I., & Raja, P. B. (2014). *Aquilaria crassna* leaves extracts – a green corrosion inhibitor for mild steel in 1 M HCl medium. *International Journal of Electrochemical Science*, *9*(2), 830–846.

Hijazi, K. M., Abdel-Gaber, A. M., & Younes, G. O. (2015). Influence of *Malus domestica* and *Caesalpinia bonducella* leaf extracts on the corrosion behaviour of mild steel in H2SO4 solution. *International Journal of Electrochemical Science*, *10*(6).

Ikeuba, A. I., John, O. B., Bassey, V. M., Louis, H., Agobi, A. U., Ntibi, J. E., & Asogwa, F. C. (2022). Experimental and theoretical evaluation of Aspirin as a green corrosion inhibitor for mild steel in acidic medium. *Results in Chemistry*, *4*. https://doi.org/10.1016/j.rechem.2022.100543

Ikeuba, A. I., Okafor, P. C., Ekpe, U. J., & Ebenso, E. E. (2013). Alkaloid and non-alkaloid ethanolic extracts from seeds of *Garcinia kola* as green corrosion inhibitors of mild steel in H2SO4 solution. *International Journal of Electrochemical Science*, *8*(5), 7455–7467.

Jafari, H., Danaee, I., Eskandari, H., & Rashvandavei, M. (2013). Electrochemical and quantum chemical studies of *N, N'-bis (4-hydroxybenzaldehyde)-2, 2-dimethylpropandiimine* Schiff base as corrosion inhibitor for low carbon steel in HCl solution. *Journal of Environmental Science and Health, Part A*, *48*(13), 1628–1641.

Kumar, S. R. S., Shastri, S. L., Venkatesh, R., Pradeepa, K., & Krishna, V. (2019). Antibacterial potential of *Caesalpinia bonducella* extracts and their isolated phytoconstituents: In vitro and in silico analysis. *Journal of Applied Biology and Biotechnology*, *7*(3). https://doi.org/10.7324/JABB.2019.70308

Loto, R. T., Mbah, E. H., & Ugada, J. I. (2021). Corrosion inhibition effect of *Citrus sinensis* essential oil extract on plain carbon steel in dilute acid media. *South African Journal of Chemical Engineering*, *35*. https://doi.org/10.1016/j.sajce.2020.08.004

Miralrio, A., & Espinoza Vázquez, A. (2020). Plant extracts as green corrosion inhibitors for different metal surfaces and corrosive media: a review. *Processes*, *8*(8), 942.

Musah, M., Azeh, Y., Mathew, J. T., Umar, M. T., Abdulhamid, Z., & Muhammad, A. I. (2022). Adsorption kinetics and isotherm models: a review. *CaJoST*, *4*(1), 20–26.

Nallagouni, C. S. R., Gangapuram, B. R., & Karnati, P. R. (2021). Green synthesis of gold nanoparticles using leaf extract of

https://doi.org/10.51459/jostir.2025.1.1.04

Caesalpinia bonducella and its biological applications. *Research Journal of Pharmacy and Technology*, *14*(2). https://doi.org/10.5958/0974-360X.2021.00185.2

Nazeerullah, K., Sunil, K., Pal, S. R., & Neelam, D. (2012). A pharmacognostic and pharmacological overview on *Caesalpinia bonducella*. In *Research Journal of Pharmaceutical, Biological and Chemical Sciences* (Vol. 3, Issue 1, pp. 440–496).

Ng, J. H., Almubarak, T., & Nasr-El-Din, H. (2022). Natural alkaloid as a non-toxic, environmentally friendly corrosion inhibitor. *The Canadian Journal of Chemical Engineering*, *100*(6), 1214–1225.

Oladipo, B., Govender-Opitz, E., & Ojumu, T. V. (2021). Kinetics, Thermodynamics, and Mechanism of Cu (II) Ion Sorption by Biogenic Iron Precipitate: Using the Lens of Wastewater Treatment to Diagnose a Typical Biohydrometallurgical Problem. *ACS Omega*, *6*(42), 27984–27993. https://doi.org/10.1021/ACSOMEGA.1C03855

Olasehinde, E. F., Agbaffa, B. E., Adebayo, M. A., & Enis, J. (2022). Corrosion protection of mild steel in acidic medium by titanium-based nanocomposite of *Chromolaena odorata* leaf extract. *Materials Chemistry and Physics*, *281*, 125856.

Olasehinde, E. F., Agbaffa, E. B., Adebayo, M. A., & Abata, E. O. (2022). Corrosion Inhibition of Mild Steel in 1 M HCl by Methanolic *Chromolaena odorata* Leaf Extract: Experimental and Theoretical Studies. *Journal of Bio-and Tribo-Corrosion*, *8*(4), 105.

Olasehinde, E. F., Ogunjobi, J. K., Akinlosotu, O. M., & Omogbehin, S. A. (2015). Investigation of the Inhibitive Properties of *Alchornea laxiflora* leaves on the Corrosion of Mild Steel in HCl: Thermodynamics and Kinetic Study.

Olivares, O., Likhanova, N. V., Gomez, B., Navarrete, J., Llanos-Serrano, M. E., Arce, E., & Hallen, J. M. (2006). Electrochemical and XPS studies of decylamides of α-amino acids adsorption on carbon steel in acidic environment. *Applied Surface Science*, *252*(8), 2894–2909.

Pradeep Kumar, C. B., & Mohana, K. N. (2014). Phytochemical screening and corrosion inhibitive behavior of *Pterolobium hexapetalum* and *Celosia argentea* plant extracts on mild steel in industrial water medium. *Egyptian Journal of Petroleum*, *23*(2). https://doi.org/10.1016/j.ejpe.2014.05.007

Salleh, S. Z., Yusoff, A. H., Zakaria, S. K., Taib, M. A. A., Abu Seman, A., Masri, M. N., Mohamad, M., Mamat, S., Ahmad Sobri, S., Ali, A., & Teo, P. Ter. (2021). Plant extracts as green corrosion inhibitor for ferrous metal alloys: A review. In *Journal of Cleaner Production* (Vol. 304). https://doi.org/10.1016/j.jclepro.2021.127030

Sathiya, S., Bharathi, K., & Geetha, S. (2014**).** *Datura Metal* as a Potential Corrosion Inhibitor for Aluminium in 1M HCl solution. *Journal of Environmental Nanotechnology*, *3*(1), 1–8.

Sehmi, A., Ouici, H. B., Guendouzi, A., Ferhat, M., Benali, O., & Boudjellal, F. (2020). Corrosion inhibition of mild steel by newly synthesized pyrazole carboxamide

https://doi.org/10.51459/jostir.2025.1.1.04

derivatives in HCl acid medium: experimental and theoretical studies. *Journal of the Electrochemical Society*, *167*(15), 155508.

Shukla, S., Mehta, A., John, J., Mehta, P., Vyas, S. P., & Shukla, S. (2009). Immunomodulatory activities of the ethanolic extract of *Caesalpinia bonducella* seeds. *Journal of Ethnopharmacology*, *125*(2). https://doi.org/10.1016/j.jep.2009.07.002

Shukla, S., Mehta, A., Mehta, P., Vyas, S. P., Shukla, S., & Bajpai, V. K. (2010). Studies on anti-inflammatory, antipyretic and analgesic properties of *Caesalpinia bonducella* F. seed oil in experimental animal models. *Food and Chemical Toxicology*, *48*(1). https://doi.org/10.1016/j.fct.2009.09.015

Singh, A., Ahamad, I., Singh, V. K., & Quraishi, M. A. (2011). Inhibition effect of environmentally benign *Karanj (Pongamia pinnata)* seed extract on corrosion of mild steel in hydrochloric acid solution. *Journal of Solid State Electrochemistry*, *15*(6). https://doi.org/10.1007/s10008-010-1172-z

Singh, A. K., Mohapatra, S., & Pani, B. (2016). Corrosion inhibition effect of *Aloe Vera* gel: gravimetric and electrochemical study. *Journal of Industrial and Engineering Chemistry*, *33*, 288–297.

Thommes, M., Kaneko, K., Neimark, A. V., Olivier, J. P., Rodriguez-Reinoso, F., Rouquerol, J., & Sing, K. S. W. (2015). Physisorption of gases, with special reference to the evaluation of surface area and pore size distribution (IUPAC Technical Report). *Pure and Applied Chemistry*, *87*(9–10). https://doi.org/10.1515/pac-2014-1117

Umoren, S. A., Eduok, U. M., Solomon, M. M., & Udoh, A. P. (2016). Corrosion inhibition by leaves and stem extracts of *Sida acuta* for mild steel in 1 M H2SO4 solutions investigated by chemical and spectroscopic techniques. *Arabian Journal of Chemistry*, *9*. https://doi.org/10.1016/j.arabjc.2011.03.008

Umoren, S. A., Solomon, M. M., Obot, I. B., & Suleiman, R. K. (2018). Comparative studies on the corrosion inhibition efficacy of ethanolic extracts of date palm leaves and seeds on carbon steel corrosion in 15% HCl solution. *Journal of Adhesion Science and Technology*, *32*(17). https://doi.org/10.1080/01694243.2018.1455797

Verma, C., Ebenso, E. E., Bahadur, I., & Quraishi, M. A. (2018). An overview on plant extracts as environmental sustainable and green corrosion inhibitors for metals and alloys in aggressive corrosive media. *Journal of Molecular Liquids*, *266*, 577–590.

Verma, C., Olasunkanmi, L. O., Ebenso, E. E., Quraishi, M. A., & Obot, I. B. (2016). Adsorption Behavior of Glucosamine Based Pyrimidine-Fused Heterocycles as Green Corrosion Inhibitors for Mild Steel: Experimental and Theoretical Studies. *The Journal of Physical Chemistry C*, *120*, 11598–11611.

Wang, D., Li, Y., Chen, B., & Zhang, L. (2020). Novel surfactants as green corrosion inhibitors for mild steel in 15% HCl: Experimental and theoretical studies. *Chemical Engineering Journal*, *402*. https://doi.org/10.1016/j.cej.2020.126219

https://doi.org/10.51459/jostir.2025.1.1.04